Thalamic model of awake alpha oscillations and implications for stimulus processing

Sujith Vijayan[1] and Nancy J. Kopell[1]

Department of Mathematics and Statistics, Boston University, Boston, MA 02215

We describe a unique conductance-based model of awake thalamic alpha and some of its implications for function. The full model includes a model for a specialized class of high-threshold thalamo-cortical cells (HTC cells), which burst at the alpha frequency at depolarized membrane potentials (~-56 mV). Our model generates alpha activity when the actions of either muscarinic acetylcholine receptor (mAChR) or metabotropic glutamate receptor 1 (mGluR1) agonists on thalamic reticular (RE), thalamocortical (TC), and HTC cells are mimicked. In our model of mGluR1-induced alpha, TC cells are equally likely to fire during any phase of alpha, consistent with in vitro experiments. By contrast, in our model of mAChR-induced alpha, TC cells tend to fire either at the peak or the trough of alpha, depending on conditions. Our modeling suggests that low levels of mGluR1 activation on a background of mAChR agonists may be able to initiate alpha activity that biases TC cells to fire at certain phases of alpha, offering a pathway for cortical control. If we introduce a strong stimulus by increasing the frequency of excitatory post-synaptic potentials (EPSPs) to TC cells, an increase in alpha power is needed to mimic the level of phasing of TC cells observed in vivo. This increased alpha power reduces the probability that TC cells spike near the trough of alpha. We suggest that mAChR-induced alpha may contribute to grouping TC activity into discrete perceptual units for processing, whereas mGluR1-induced alpha may serve the purpose of blocking unwanted stimuli from reaching the cortex.

Alpha rhythms (8–13 Hz) were first observed in humans over the occipital cortex by Berger (1), when subjects were in a relaxed state with their eyes closed. Occipital alpha has been investigated extensively since. However, alpha rhythms are not strictly confined to this area of cortex; alpha activity has also been reported in the somatosensory cortex (2), the auditory cortex (3), and the prefrontal cortex (4).

Both the neural substrates responsible for the genesis of alpha and its functional role in cognition remain hotly debated. At the functional level, the point of contention is whether alpha activity serves to process information relevant to the task at hand or serves to filter out irrelevant information. The debate over where alpha activity is generated primarily revolves around whether it is generated by the neocortex, by the thalamus, or by a combination of the two. We make use of recent findings (5–10), as well as prior findings (11–17), to construct a unique conductance-based thalamic model of awake alpha, and use it to address the above controversy.

Studies have found that during simultaneous in vivo recordings from the thalamus and neocortex, alpha activity in the neocortex is accompanied by alpha rhythms in the local field potential of the thalamus and in the firing patterns of individual thalamocortical (TC) cells (5, 18). During alpha activity, only 10–30% of TC cells fire in the alpha frequency (5, 6). Their firing pattern consists of high-threshold bursts (HTBs), with the intervals between bursts occurring at the alpha frequency, and gap junctions play a critical role in synchronizing their activity (10). Alpha activity can be induced in thalamic slices in the presence of metabotropic glutamate receptor (mGluR1) agonists (5) or muscarinic acetylcholine receptor (mAChR) agonists (8). As in the in vivo case, only a small fraction of TC cells exhibits HTB at the alpha frequency in the presence of mGluR1 and mAChR agonists. Although the mechanisms by which mGluR1 agonists and mAChR agonists

induce HTB may differ, they both seem to do so, in part, by reducing potassium leak conductances and by activating an I_T channel that acts at more depolarized membrane potentials than the standard I_T channel (7).

For our model, we developed two submodels: one for a specialized class of high-threshold thalamocortical cells (HTC cells) and one for an I_T-channel variant suggested to play a critical role in the generation of thalamic alpha (5–7, 17). We denote by I_{TLT} and I_{THT} the calcium currents associated with the low- and high-threshold variants, respectively. The model generates alpha activity upon choosing parameters to reflect the presence of either mGluR1 or mAChR, consistent with experimental data (5–9). We show that mGluR1- and mAChR-mediated alpha rhythms produce differential effects on the firing of TC cells with respect to the alpha rhythm, and discuss the functional implications.

Methods

The model presented here was constructed with the objective of capturing the physiological features of thalamic alpha. Our model consists of single-compartment Hodgkin–Huxley neurons. The membrane potential of each cell is governed by the equation

$$C_M \frac{dV}{dt} = -\sum I_M - \sum I_{syn}.$$

Here, I_M denotes the membrane currents, I_{syn} denotes synaptic currents, and C_M denotes the specific membrane capacitance.

The thalamic model developed by Destexhe et al. (16), which consists of a network of reticular (RE) nucleus cells and TC cells, was used as a starting point for our model; the parameters of this model were used unless otherwise specified. We incorporated into this model a specialized subset of TC cells, called HTC cells, which are connected by gap junctions (10) and can fire HTBs (Fig. 1A). The coupling via the gap junction is relatively weak and serves to keep the HTC cells synchronized. The percentage of HTC cells in the total population of TC cells was kept to between 15 and 25%, in keeping with experimental findings (5, 6). All three cell types contain a leak current (I_L), a potassium leak current (I_{KL}), a sodium current (I_{Na}), a potassium current (I_K), and an applied current (I_{app}) (SI Methods). The applied current consists of baseline current with Gaussian noise and/or a Poisson train of EPSPs and/or IPSPs (SI Methods and Table S1). All three contain two variations of a low-threshold calcium current as well (I_{TRE}, I_{TLT}). The two types of TC cells also contain a hyperpolarization-activated cation current (I_H), with the equations governing this current in HTC cells altered such that the graph is shifted by 15 mV to the right (SI Methods; also 13, 15). HTC cells also contain three additional currents: (I_{AHP}), a calcium-activated potassium current, (I_{THT}), a high-threshold calcium current, and I_{GJ}, the current passed via gap junctions (SI Methods).

In this model the RE cells provide inhibition to both TC and HTC cells, mediated by both GABA$_A$ and GABA$_B$, and also inhibition to each other, mediated by GABA$_A$. The TC and HTC cells in turn provide excitatory inputs (AMPA) to the RE cells (Fig. 1A; SI Methods). Local interneurons are found in many thalamic nuclei and play a prominent role in thalamic alpha. Whereas these local interneurons receive external inputs, they also receive excitatory inputs from HTC cells and in turn inhibit TC cells (9). The thalamic

NEUROSCIENCE

APPLIED MATHEMATICS
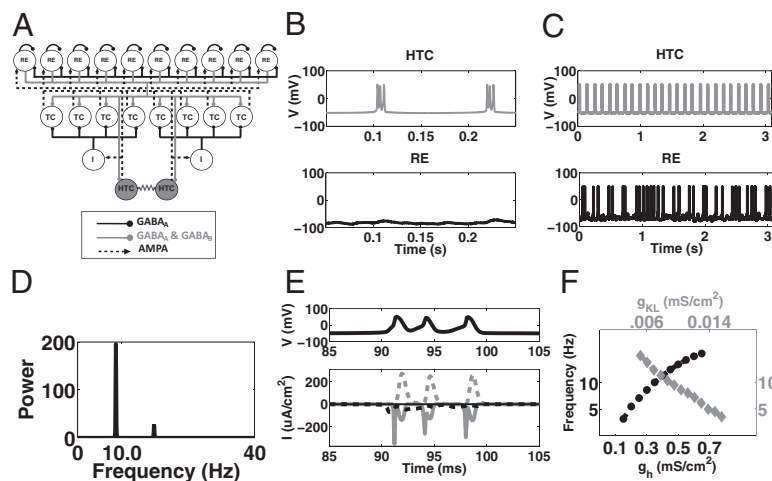
Fig. 1. Network architecture of thalamic alpha model, and description of mAChR- and mGluR1-induced alpha. (*A*) Network consists of RE cells, TC cells, thalamic interneurons (I), and a specialized subset of TC cells, called HTC cells, which are connected by gap junctions. The interneurons are implicit in our model; that is, we include direct inhibitory connections between HTC cells and TC cells in place of the connections via the thalamic interneurons. (*B*) Example of HTC cell activity (*Upper*) and RE cell activity (*Lower*) during mAChR-induced alpha. (*C*) Same as *B*, but during mGluR1-induced alpha. Notice the arrhythmic spiking pattern of the RE cell. (*D*) Power spectrum of LFP (see *SI Methods* for definition) generated in the example shown in *B*. (*E*) (*Upper*) Burst consisting of three spikes during mAChR-induced alpha. (*Upper*) Potassium current (dotted gray trace), sodium current (solid gray trace), I_{THT} (dotted black trace), I_{TLT} (solid black trace) during burst shown on top. (*F*) During mAChR-induced alpha the frequency of bursts produced by HTC cells, and therefore the frequency of the LFP oscillations, increases as the maximal I_H conductance is increased (black dotted trace and black axes) or as the maximal I_{KL} conductance is decreased (gray trace and gray axes).

interneurons are implicit in our model: we bypass the interneurons by introducing a direct inhibitory connection from the HTC cells to the TC cells. More explicitly, the interneurons fire either in single-spike mode or in burst mode (9); they enter burst mode when they are more depolarized. Bursting mode consists of a single spike followed by a train of up to eight spikes with an interspike interval between the first and second spike of ~35.5 ms (9). To model the bursting mode of interneurons, we added a delay in the release of GABA$_A$, because the inhibition onto TC cells from interneurons in bursting mode occurs at a later time relative to that from interneurons in single-spike mode (9). That is, in our model, during single-spike mode there is no delay in the inhibition from HTC cells to TC cells, whereas in burst mode there is a 40-ms delay. When interneurons burst they provide a delayed inhibition onto the TC cells. We believe that the mechanisms underlying the burst are not germane to how the network uses the delayed inhibition, and the mechanisms underlying this delay are not well understood.

For mGluR1 conditions we lowered the leak conductances of RE, TC, and HTC cells, whereas for mAChR conditions we lowered it only for TC and HTC cells. Under both mGluR1 and mAChR conditions TC cells receive a Poisson train of EPSPs. This Poisson train to the TC cells serves as the stimulus in all conditions aside from the transient stimulus condition. Additional information is in *SI Note 1: mAChR Model Properties, SI Note 2: mGluR1 Model Properties*, and Table S1. In vivo and in vitro studies suggest that these HTC cells burst at the alpha frequency at depolarized background membrane potentials greater than −60 mV (5, 6). The bursts are thought to be mediated by a variant of an I_{TLT} channel, a type of calcium channel, which operates at more depolarized membrane potentials than does the standard I_{TLT} channel (5–7, 17). To incorporate such a channel, which we call I_{THT}, we started with the activation and inactivation functions of a standard I_{TLT} channel and shifted both curves to the right by ~25 mV. This results in a shift of their point of intersection to a more depolarized value. As a result, I_{THT} channels have a greater conductance in comparison with standard I_{TLT} channels when the membrane potential is held at relatively depolarized values (e.g., −55 mV) (Fig. S1A). The number of spikes per burst during thalamic alpha in vivo and in vitro ranges from 1 to 4; this is fewer than the number of spikes that occur during bursts mediated by the standard I_{TLT} channel (6). To reduce the number of spikes per burst we altered the slopes of the activation and inactivation functions by changing the slope factor term of the Boltzmann function. The function [h$_t$(V); *Methods*] that determines the time constants of inactivation was shifted as well, so that its values were smaller at membrane potentials near −60 mV (Fig. S1B). In addition to the shift, time constant values were increased at hyperpolarized membrane potentials, so that the channel tended to be inactive at hyperpolarized membrane potentials. That is, the time constants were altered such that the channel tended to deinactivate more quickly at depolarized

membrane potentials (e.g., −60 mv) but more slowly at relatively hyperpolarized membrane potentials (e.g., −90 mv) than standard I_{TLT} channels.

Results

Cholinergically (mAChR)-Induced Alpha. Metabotropic cholinergic agonists can induce alpha oscillations in thalamic slices (8). Experimental studies suggest that mAChR agonists hyperpolarize RE cells by increasing their potassium leak conductance (12) and depolarize TC cells by decreasing potassium leak conductances (13). When these actions of mAChR agonists are accounted for in our model (*Methods*), the HTC cells burst at the alpha frequency (Fig. 1 *B, Upper* and *D*). Note that the RE cells are silent, consistent with slice studies (9). TC cells are active during mAChR-induced thalamic alpha activity. Their activity pattern is discussed in detail in *Phasing: TC Firing in Relation to Alpha Oscillations*.

The I_{THT} channels play a prominent role in the bursting of the HTC cells. Observe that during a high threshold burst (black trace, Fig. 1E, *Upper*), I_{THT} channels are active before each burst (dotted black trace, Fig. 1E, *Lower*) whereas I_{TLT} channels (solid black trace, Fig. 1E, *Lower*) are relatively quiet. The I_{TLT} channels are quiet because they are inactive at such depolarized membrane potentials. Decreasing I_{KL} conductance depolarizes HTC cells and increases the frequency of HTC bursts, whereas decreasing I_H conductance does the opposite (Fig. 1F). I_H also plays a role in the initiation of each burst.

Glutamergically (mGluR1)-Induced Alpha. Experimental studies suggest that glutamate agonists depolarize TC cells, just as mAChR does. However, unlike mAChR, glutamate agonists depolarize RE cells as well. When the actions of mGluR1 are accounted for in our model (*Methods*), HTC cells burst at the alpha frequency (Fig. 1C, *Upper*) and Fig. S2A); observe that the scale in Fig. 1C is different from that in Fig. 1B. Under these conditions RE cells are active (Fig. 1C, *Lower*). TC cells are active during mGluR1-induced alpha as well. See *Phasing* for their pattern of activity. The frequency of mGluR1-induced oscillations increases as the I_H conductance is increased or as the I_{KL} conductance is decreased (Fig. S2B). Although the results described here use a Poisson train of EPSPs as
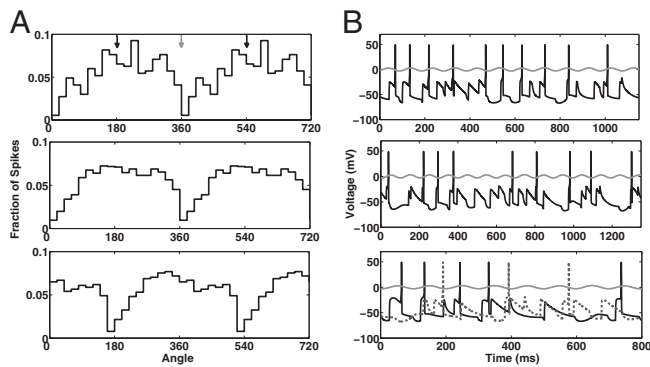
Fig. 2. TC cell activity during mAChR-induced alpha with interneurons in single-spike mode or burst mode. (*A*) (*Top*) Fraction of total spikes that occur at a particular phase of alpha for a single TC cell when interneurons are in single-spike mode. The *x* axis has been extended to 720°. The black arrows at the top indicate the angle that corresponds to the peak of the alpha oscillation; the gray arrow indicates the angle that corresponds to the trough. The TC cell tends to fire near the peak of alpha. (*Middle*) Same as *Top*, but for total spikes for all TC cells. (*Bottom*) Same as *Middle*, but interneurons are in burst mode. (*B*) (*Top*): Spiking activity of a single TC cell relative to the LFP (gray trace) with interneurons in single-spike mode. Note that although the TC cell tends to fire near the peak of the alpha oscillation it does not always do so (e.g., see the first and fifth spikes). (*Middle*) Same as *Top*, but interneurons are in burst mode. Note that although the TC cell tends to fire near the trough of the alpha oscillation it does not always do so (e.g., see the first spike). (*Bottom*) Spiking activity of two individual TC cells, relative to LFP, when some interneurons are in single-spike mode and others are in burst mode. The TC cell receiving input from an interneuron in single-spike mode (black trace) tends to fire near the peak of alpha; the TC cell receiving input from an interneuron in burst mode (dotted gray trace) tends to fire near the trough of alpha.

an ongoing stimulus, this input is not necessary to generate alpha oscillations.

Phasing: TC Firing in Relation to Alpha Oscillations. *mAChR-produced phasing of TC cells.* In our mAChR-induced thalamic alpha model, TC cells fire locked to alpha. The phase depends on the mode of the interneurons (*Methods*). When all interneurons are in single-spike mode, individual TC cells tend to fire near the peak of alpha (Fig. 2 *A* and *B*, *Top*; Rayleigh's test, $P = 3.3 \times 10^{-7}$). This pattern becomes more apparent when the spiking activity of all TC cells is considered (Fig. 2*A*, *Middle*; Rayleigh's test, $P = 1.7 \times 10^{-48}$).

When we adjust our model such that our implicit interneurons are in burst mode, individual TC cells tend to fire near the trough of alpha (Fig. 2*B*, *Middle* and Fig. S3; Rayleigh's test, $P = 4.7 \times 10^{-7}$). This becomes more evident when the spiking activity of all of the TC cells is considered (Fig. 2*A*, *Bottom*; Rayleigh's test, $P = 7.2 \times 10^{-46}$). When some of the interneurons are firing in single-spike mode and other interneurons are firing in burst mode, those TC cells receiving input from interneurons firing in single-spike mode tend to fire near the peak of alpha (black trace, Fig. 2*B*, *Middle*) whereas those receiving input from interneurons that are bursting tend to fire near the trough of alpha (dotted gray trace, Fig. 2*B*, *Bottom*). The behavior of the network in both single-spike mode and burst mode faithfully reproduces the experimental results (9). The HTC cells drive interneurons, which inhibit TC cells phasically. This inhibition occurs at the trough of the alpha oscillation in single spike mode but at the peak in burst mode, because the inhibition is delayed. The delay of the inhibition onto TC cells is the key factor determining phase.

We next examined how increasing the rate of EPSPs of the Poisson train, the ongoing stimulus, would change the phasing of the TC cells. Our rationale is that, in vivo, a stronger stimulus may result in a higher rate of EPSPs. As expected, when the rate of EPSPs

is increased, the phasing of TC cells becomes less pronounced (Fig. 3*A*, *Left*). However, as a stimulus increases in strength the brain may recruit more HTC neurons into "alpha mode" by releasing more mAChR; increasing the number of HTC cells increases the extent to which TC cells are phased, for a given rate of EPSPs (Fig. 3*A*, *Right*). Via the interneurons, the HTC cells increase the phasic inhibition onto the TC cells and therefore restrict the spiking of TC cells to a smaller window. As more HTC cells are recruited, the alpha power increases (Fig. 3*B*).

We have been considering the phasing of TC cells firing in response to a sustained Poisson train of EPSPs. Using our model we also sought to characterize the phasing of TC cells that are firing in response to transient stimuli over a background of mAChR-induced alpha (19–24). The transient stimulus was modeled as a rectangular current pulse input to TC cells (*SI Methods*). We observed the time at which TC cell spiking occurred relative to the time of onset of stimulus presentation. We used several different stimulus strengths. First, we used a 4-μA/cm², 10-ms stimulus, which, in the absence of alpha activity, is just below the threshold necessary to produce spiking activity in TC cells. During mAChR-induced alpha activity, we find that TC cells do not fire when the stimulus is presented during the trough of alpha activity, but do fire when the stimulus is presented at or around the peak of alpha activity (black circles, Fig. 3*C*, *Left*), as we expected. If we increase the duration of the stimulus to 100 ms but keep the amplitude of the stimulus at 4 μA/cm², we find that TC cells spike regardless of the phase at which the stimulus is presented (gray circles, Fig. 3*C*, *Left*).

When we further reduce the amplitude of the stimulus to 1.35 μA/cm², TC cells do not spike for a stimulus that is of 10-ms duration, but do spike for a 50-ms stimulus (black circles, Fig. 3*C*, *Right*). Surprisingly, TC cells spike only if the stimulus onset occurs
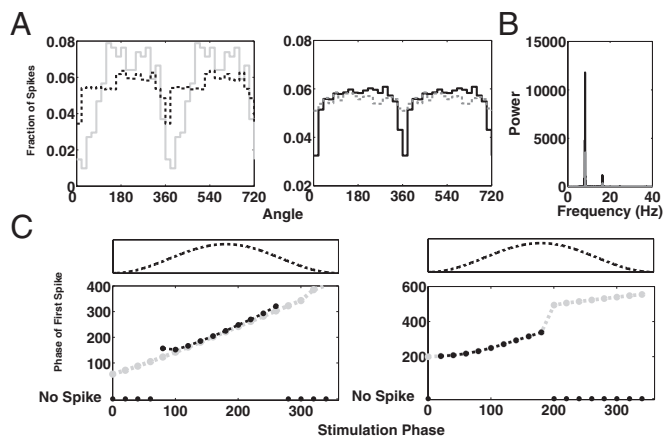
Fig. 3. Phasing of TC cells during mAChR-induced alpha. (*A*) (*Left*) Spiking activity of the TC cell population as a function of the phase of alpha, given a 20-Hz Poisson train of EPSPs to TC cells (gray trace) or given a 200-Hz Poisson train of EPSPs to TC cells (black dashed trace). (*Right*) In the presence of a 100-Hz Poisson train of EPSPs, the recruitment of more HTC cells (six cells vs. two cells) phases TC cells to a greater extent (black trace, six HTC cells, Rayleigh's test, $P = 1.45 \times 10^{-41}$ vs. gray trace, two HTC cells, Rayleigh's test, $P = 8.32 \times 10^{-4}$). Note that in making the network, larger parameters had to be adjusted, resulting in overall less phasing in all conditions than in the *Left*. (*B*) Recruitment of additional HTC cells results in greater alpha power. Gray/black same as in *A*, *Right*. (*C*) (*Left*) Phase of alpha at which the first spike occurred as a function of the phase of alpha at which the onset of the transient stimulus occurred. Transient stimulus is a rectangular current pulse, 10 ms (black trace) or 100 ms (gray trace) in duration and 4 μA/cm² in amplitude. Circles at the bottom indicate that no spike occurred in response to the stimulus. The dotted trace above represents one alpha cycle. (*Right*) Same as in *Left* but using a rectangular current pulse, 50 ms (black trace) or 100 ms (gray trace) in duration and 1.35 μA/cm² in amplitude.

when the alpha oscillation is transitioning from trough to peak (40–180°), but not when it is transitioning from peak to trough. If the stimulus is made longer but the amplitude is kept the same (1.35 μA/cm^2, 100 mS), the TC cells spike at all of the phases of alpha (gray circles, Fig. 3C, *Right*). When the stimulus is presented during a transition from peak to trough, the spike occurs during the following cycle of the alpha oscillation, during the transition from trough to peak. As expected, our results suggest that when a transient stimulus is strong, but not strong enough to produce spiking activity during all phases of alpha, TC cells will preferentially fire when inhibition is lowest during the alpha cycle. Also, our results suggest that for a sufficiently weak stimulus, TC cells not only preferentially spike in response to a stimulus that is presented when inhibition is lowest, but they prefer a stimulus initially presented when inhibition is decreasing. This is because, if the stimulus onset occurs when the alpha oscillation is transitioning from peak to trough, the point at which the TC cell would normally spike coincides with a period of maximal inhibition from the thalamic interneurons.

mGluR1 does not induce phasing of TC cells. During mGluR1-induced thalamic alpha, TC cells do not show a preference for firing at a particular phase of alpha, and both RE cells and thalamic interneurons fire irregularly (9). Lorincz et al. (9) suggest that irregular firing of RE cells may be primarily responsible for the lack of TC cell phasing. Because both RE cells and thalamic interneurons receive inputs from HTC cells, which spike at the alpha frequency during mGluR1-induced thalamic alpha, both RE cells and interneurons could in theory be driven rhythmically. In turn, RE cells or thalamic interneurons could inhibit TC cells in a rhythmic fashion, thus biasing the phase of alpha at which TC cells fire. Therefore, there are potentially at least two pathways that could phase the firing of TC cells: via RE cells or thalamic interneurons. Our model shows that it is important that both populations of cells fire in an irregular fashion to ensure that TC cells are not biased to fire during a particular phase of alpha (*SI Note 3: Role of Interneurons and RE Cells During mGluR1-Induced Alpha*; Fig. S4). If both the interneurons and RE cells fire irregularly, then the TC cells are not phased (Fig. 4A, *Lower Left*; Rayleigh's test, P = 0.75).

mGluR1 offers a means for cortical control. It is known that thalamic mGluR1 receptors can be activated by cortical inputs. This pathway offers a potential means of cortical control of mAChR-induced alpha during cognitive tasks. We considered the possibility that mGluR1 may act to modulate alpha activity in the presence of mAChR agonists: because both mGluR1 and mAChR act on potassium leak conductances of HTC cells, HTC cells that are on the cusp of oscillating in the presence of mAChR might be pushed to oscillate by mGluR1. Furthermore, the phasing of TC cells may remain intact under such low doses of mGluR1. To test this idea, we adjust our parameters to those used for mAChR-induced alpha, with the exception that we do not reduce the potassium leak

conductances as much as we normally would (*Methods* and *SI Methods*). Then, HTC cells are relatively depolarized but do not oscillate (Fig. S5, *Left*). We then adjust the parameters of our model to introduce a low level of mGluR1 (*Methods* and *SI Methods*). HTC cells then oscillate at the alpha frequency (Fig. S5, *Right*). Furthermore, at such low doses of mGluR1 TC cells are still phased (Fig. 4B, *Lower Right*; Rayleigh's test, P = 1.6 × 10^{-4}).

Discussion

Overview of Results. There is ongoing controversy concerning whether the alpha rhythm is produced in the thalamus or the neocortex, or whether both structures contribute (5, 6, 9, 18, 19, 23, 25–27). Here, we present a Hodgkin–Huxley-based model of awake thalamic alpha. In constructing our model, we developed a model for a specialized class of HTCs, which burst at the alpha frequency at depolarized membrane potentials (∼−56 mV). In the process of making this cell, we developed a model channel, I$_{THT}$, which can generate HTBs similar to those that have been observed during thalamic alpha in vivo and in vitro (5–7, 17). These I$_{THT}$ channels have properties similar to standard I$_{TLT}$ channels but they operate at more depolarized membrane potentials; Williams and Stuart (17) demonstrate that such channels exist.

Our model generates alpha activity if parameters are chosen to reflect the actions of either mAChR or mGluR1 on RE, TC, and HTC cells. We observe that in our model of mGluR1-induced alpha, TC cells are equally likely to fire during any phase of alpha, consistent with in vitro experiments. Our model suggests that in order for TC cells to fire in such a fashion, it is necessary that the firing patterns of both RE cells and thalamic interneurons be irregular. By contrast, in our model of mAChR-induced alpha, TC cells fire phase-locked to alpha. Specifically, those TC cells receiving input from interneurons in single-spike mode tend to fire at the peak of the alpha oscillation (Fig. 2A, *Middle*), whereas those TC neurons receiving input from interneurons in burst mode tend to fire at the trough of alpha (Fig. 2A, *Bottom*).

TC Signaling During mAChR-Induced Alpha. To determine how the phasing of TC neurons during mAChR-induced alpha might influence how TC cell activity induces activity in the cortex, we need an understanding of the relationship between thalamic alpha and simultaneous activity in the neocortex. There are several clues as to what this relationship might be. Work by Lörincz et al. (9) [see figure 1 a and b in ref. 9] suggests that alpha activity in the visual thalamus (LGN) is in phase with alpha activity detected in the EEG above the visual cortex. Bollimunta et al. (23) [see discussion and supplemental figures in ref. 23] found that alpha activity in the LGN is coherent with alpha activity only in the superficial layers of the visual cortex, but not in deeper layers [local field potential (LFP) traces in Fig. 5A]. Thus, the studies by Lörincz et al. (9) and Bollimunta et al. (23) taken together suggest that the alpha oscillations in the superficial layers of the neocortex and in the LGN are in phase, with zero lag (LFP traces in Fig. 5A).

In *SI Note 4: Details of TC Signaling During mAChR-Induced Alpha*, we argue that various data about multiunit activity and phasing can be explained if HTC cells project to superficial layers, as do cells from the matrix, synapsing onto interneurons that in turn inhibit pyramidal cells in layer 4 (Fig. 5B). Because thalamic alpha and superficial neocortical alpha are in phase, TC cells that fire at the peak of thalamic alpha (i.e., out of phase with HTC cells), might be better able to drive layer IV cells, because their output occurs when inhibition from superficial neocortical interneurons is minimal (Fig. 5A). Because the TC cells that fire during the trough of thalamic alpha are the ones that receive inputs from interneurons in burst mode i.e., more depolarized interneurons (*Methods*)], TC cells receiving inputs from depolarized interneurons might be less effective in driving cortical neurons because their output occurs when inhibition to their targets from neocortical interneurons is maximal.
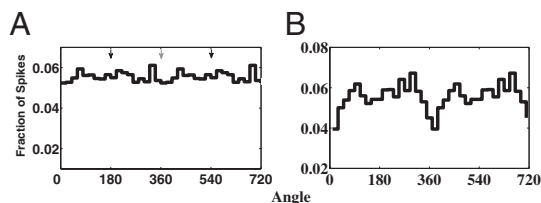
Fig. 4. TC cell activity during mGluR1-induced alpha and during low levels of mGluR1 agonists on a background of mAChR agonists. (*A*) TC cell population spiking activity when both interneuron and RE cell activity is arrhythmic. Spiking activity is not phased (Rayleigh's test, P = 0.75). (*B*) TC cell population spiking activity with low levels of mGluR1 agonists on background of mAChR agonists. Spiking activity is phased (Rayleigh's test, P = 1.6 × 10^{-4}), with cells tending not to fire near the peak of alpha.

Vijayan and Kopell

Fig. 5. Cartoon and circuit diagram illustrating the possible TC interactions during alpha oscillations. (*A*) Cartoon of simultaneous alpha oscillations in the neocortex and thalamus, and the relative strength of neocortical multiunit activity and thalamic single-unit activity in relation to the alpha oscillations. The cartoon is based on findings reported in Bollimunta et al. (23) and Lörincz et al. (3), which suggest that the alpha oscillations only in the superficial layers of the neocortex (gray trace, *Upper*) are in register with the alpha oscillations in the thalamus (gray trace, *Lower*). In the superficial layers of the neocortex, multiunit activity is greatest during the trough of alpha (gray arrows), whereas in layer IV it is greatest during the peak of alpha (black arrows). In the thalamus (*Lower*) both the HTC cells and those TC cells receiving input from interneurons in burst mode tend to spike near the trough of alpha, whereas those TC cells receiving input from interneurons in single-spike mode tend to fire near the peak of alpha. (*B*) Circuit diagram of one pathway by which thalamic alpha may influence which spikes from TC cells are able to drive layer IV pyramidal cells (PY, granular layer). HTC cells drive interneurons (I) in the superficial layers of the neocortex, which in turn inhibit layer IV PY cells. As a consequence, a TC cell that fires right after an HTC cell fires may not be effective in driving layer IV PY cells; therefore TC cells that fire near the trough of alpha may not be as effective in driving layer 4 PY cells as TC cells that fire during the peak of alpha.
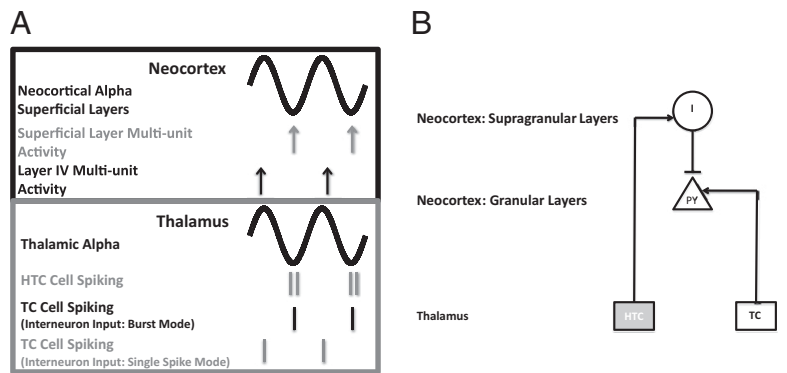
Jones et al. (19) have developed a biophysical model of the mu rhythm, a neocortical rhythm (over somatosensory cortices) that is a mixture of the alpha and beta rhythms. In their model, cortical alpha arises as a result of two distinct thalamic alphas (from lemniscal and nonlemniscal pathways) driving different layers of the cortex, with their drives offset by 50 ms. That work does not directly model the thalamic alpha; rather, it describes the consequences at the cortical level of inputs at the alpha frequency. By contrast, we are focusing on the mechanisms of the thalamic alpha and the potential consequences of the interaction between thalamic and cortical alpha. Our thinking is based on experimental data from alpha activity in the primary visual cortex, because our thalamic model is based largely on data from the LGN. Therefore, the differences in the relationship between cortical alpha and thalamic alpha suggested by us and by Jones et al. may be due to differences in the anatomic location of the two alphas. Furthermore, the alpha in the mu rhythm may be fundamentally different from the occipital alpha rhythm, as the former is often accompanied by a beta rhythm, whereas the latter is not.

During mAChR-Induced Alpha, Increased Power Helps Processing During Tasks. The functional role of alpha rhythms is hotly debated. A point of contention is whether alpha activity serves to process information relevant to the task at hand or rather serves to filter out irrelevant information. The latter hypothesis is seemingly supported by studies showing that in tasks in which subjects are asked to attend to an object on one side of their visual field, alpha power decreases on the side of the occipital cortex that processes the stimulus to be attended (23, 28, 29), whereas alpha power increases on the side that primarily processes the nonrelevant stimulus (30, 31); similar results have also been observed in the somatosensory cortex (22). Also, alpha power increases during mental arithmetic tasks (32), and increases in power with an increase in memory load during working memory tasks (33, 34); these results can easily support either hypothesis, depending on one's interpretation.

We first discuss how cholinergically induced alpha can be useful for active stimulus processing. Both in vivo and in vitro cholinergic data suggest that during thalamic alpha, TC cell spiking is phased with a relatively long duty cycle (9). Phasing may be critical for stimulus perception, acting to "chunk" stimuli into discrete perceptual units for processing (9, 35). A long duty cycle occurs in our model as a consequence of choosing parameters to reflect the known effects of mAChR on TC and RE cells; we did not adjust parameters to achieve this long duty cycle.

In our model of mAChR-induced alpha, we found that the extent to which TC cells are phased decreased as the frequency of external EPSP inputs is increased, given a fixed level of inhibitory input from thalamic interneurons (Fig. 2*A*, *Left*). In particular, TC cells have

a higher probability of spiking near the trough of the alpha cycle when provided with a higher frequency of EPSPs. It seems likely that the frequency of EPSPs received by TC cells during a stimulus increases as the strength of the stimulus increases, although to our knowledge no studies have addressed this assertion. Thus, our model predicts that during a strong stimulus, TC cells will become less strongly phased in the absence of a compensatory mechanism.

Within the framework of our model, HTC cells provide such a compensatory mechanism. In our model, in the presence of a strong stimulus, more HTC cells need to be recruited over the number engaged during a weak stimulus to obtain a level of phasing similar to that observed in in vivo and in vitro experiments, as in Lorincz et al. (9) (Fig. 2*A*, *Right*). Recruitment of HTC cells is an effective counter because more HTC cells drive more interneurons, increasing suppression of TC spiking activity and therefore better phasing TC cells. This recruitment of HTC cells results in increased alpha power (Fig. 2*B*).

Thus, our model predicts that in the presence of a stronger stimulus, increased alpha power will be observed. When there is significant alpha, the readout in layer IV neocortex has a brief period in which pyramidal cells are not firing; this corresponds to a period of high neocortical inhibition plus low drive from the TC cells. However, if the alpha is too weak, TC firing occurs throughout the cycle, and could potentially drive layer IV pyramidal cells in a more tonic manner. Our model thus suggests that cholinergic alpha power is important for creating chunking in the neocortex.

Glutamergically Induced Alpha Rhythms May Block Unwanted Stimuli. In contrast with mAChR alpha, during mGluR1 alpha, TC neurons receive irregular inhibition from RE cells and thalamic interneurons, and the firing of TC neurons is not phased with respect to alpha (9). Therefore, mGluR1 alpha may be a means by which the cortex, via its glutamergic projections onto the thalamus, prevents a coherent input from some portion of the thalamus from reaching the cortex. This possibility is in line with findings (36) that show that during cognitive tasks, the activity of RE neurons increases in those areas of the thalamus representing features to which one is not attending (mGluR1 agonists increase RE firing rates).

Glutamergic Release May Offer a Means of Cortical Control of Thalamic Alpha. Another possibility suggested by our simulations is that mGluR1 may modulate mAChR-induced alpha activity (Fig. 4). In this scenario, subcortical mAChR release places the thalamus on the cusp of generating alpha activity (Fig. 4*B*, *Left*). Because, like mAChR, mGluR1 reduces I_{KL} in HTC cells, cortical activation of mGluR1 initiates alpha oscillations in HTC cells (Fig. 4*B*, *Right*). Furthermore, such low levels of mGluR1 leave the phasing of HTC cells intact, as they only slightly depolarize RE cells (via I_{KL})

and minimally alter the interneurons (Fig. 4*A*, *Lower Right*). Thus, we suggest the possibility that in the presence of mAChR, the cortex may influence alpha activity in different ways, depending on the strength of its glutamergic inputs: when the release of mGluR1 agonists is low, there may be an induction of alpha without a disruption of TC cell phasing, whereas when the release is high, TC cell phasing may be disrupted.

It may be the case that the deployment of mAChR or mGluR1 alpha depends on the demands of the cognitive task at hand. We suggest that when the demands of the task require alpha for the active processing of a stimulus, mAChr-induced alpha will predominate. Under this regime alpha helps to chunk stimuli into discrete perceptual units for processing. However, if the demands of the task require alpha to be deployed to ignore a stimulus, we suggest that mGLuR1 alpha will predominate because, during mGluR1-induced alpha, TC cell activity is indiscriminately inhibited and thus alpha may prevent a coherent thalamic representation of a stimulus from reaching the cortex. If this theory is true we would expect alpha power to increase in those regions of the neocortex in which a stimulus to be ignored is processed. Therefore, depending on the type of alpha deployed, alpha may serve the purpose of either actively processing or ignoring a stimulus.

Relationship to Other Models. Our model, as well as spindling models (14–16, 37), generates oscillation in the alpha frequency. However, spindling is a network phenomenon and requires cells in the entire network to be relatively hyperpolarized (<-65 mV). In our model HTC cells can oscillate at the alpha frequency by themselves. As the cells become more depolarized the frequency of the alpha oscillations increases (Fig. 1*E* and Fig. S2*B*); increasing I_h and decreasing I_k conductances depolarizes TC and HTC cells.

Spindling models have also examined how spindles are generated in the cortex (38, 39) and recently have examined how local versus global spindles are generated (39). Bonjean et al. (39) argue that global spindles are generated by TC cells from the matrix and local ones are generated by TC cells from the core. These two groups of TC cells differ in their projections but not in how they generate spindles. We also suggest the possibility of a core/matrix distinction; however, in our model HTC cells and TC cells have fundamental differences in their biophysical properties.

Alpha Rhythms and Disease. As noted by Hughes and Crunelli (6), diseases such as schizophrenia, Parkinson disease, and neurogenic pain are marked by a slowing of the awake occipital alpha rhythm. By manipulating our biophysical model, one might gain insight into the pathophysiology of these diseases. For example, our model shows that if, in HTC cells, either the maximal potassium leak conductance is reduced or the I_H conductance is increased, then thalamic alpha frequency is slowed in the presence of either mGluR1 or mAChR; therefore, a pathological process that alters these conductances might explain the slowing of alpha in these diseases. Because mGluR1-induced alpha may be important in blocking out stimuli that one wants to ignore, abnormalities in mGluR1-related activity may play a role in disorders such as attention deficit hyperactivity disorder.

In summary, by capturing the physiological mechanisms underlying alpha rhythm dynamics, our model provides us with insight into the functional properties of alpha.

1. Berger H (1929) On the electroencephalogram of man. *Arch Psychiatr Nervenkr* 87:527–570.
2. Salmelin R, Hari R (1994) Spatiotemporal characteristics of sensorimotor neuromagnetic rhythms related to thumb movement. *Neuroscience* 60:537–550.
3. Tiihonen J, et al. (1991) Magnetoencephalographic 10-Hz rhythm from the human auditory cortex. *Neurosci Lett* 129:303–305.
4. Halgren E, Boujon C, Clarke J, Wang C, Chauvel P (2002) Rapid distributed fronto-parieto-occipital processing stages during working memory in humans. *Cereb Cortex* 12:710–728.
5. Hughes SW, et al. (2004) Synchronized oscillations at alpha and theta frequencies in the lateral geniculate nucleus. *Neuron* 42:253–268.
6. Hughes SW, Crunelli V (2005) Thalamic mechanisms of EEG alpha rhythms and their pathological implications. *Neuroscientist* 11:357–372.
7. Hughes SW, et al. (2008) Novel modes of rhythmic burst firing at cognitively-relevant frequencies in thalamocortical neurons. *Brain Res* 1235:12–20.
8. Lörincz ML, Crunelli V, Hughes SW (2008) Cellular dynamics of cholinergically induced alpha (8-13 Hz) rhythms in sensory thalamic nuclei *in vitro*. *J Neurosci* 28:660–671.
9. Lorincz ML, Kékesi KA, Juhász G, Crunelli V, Hughes SW (2009) Temporal framing of thalamic relay-mode firing by phasic inhibition during the alpha rhythm. *Neuron* 63:683–696.
10. Hughes SW, et al. (2011) Thalamic gap junctions control local neuronal synchrony and influence macroscopic oscillation amplitude during EEG alpha rhythms. *Front Psychol* 2:1–11.
11. McCormick DA, Prince DA (1986) ACh induces burst firing in thalamic reticular cells by activating a potassium conductance. *Nature* 319:402–405.
12. McCormick DA, Prince DA (1987) Acetylcholine causes rapid nicotinic excitation in the medial habenula, in vitro. *J Neurosci* 7:742–752.
13. Destexhe A, Babloyantz A (1993) A model of the inward current Ih and its possible role in thalamocortical oscillations. *Neuroreport* 4:223–226.
14. Destexhe A, McCormick DA, Sejnowski TJ (1993) A model for 8-10 Hz spindling in interconnected thalamic relay and reticularis neurons. *Biophys J* 65:2473–2477.
15. Golomb D, Wang XJ, Rinzel J (1994) Synchronization properties of spindle oscillations in a thalamic reticular nucleus model. *J Neurophysiol* 72:1109–1126.
16. Destexhe A, Bal T, McCormick DA, Sejnowski TJ (1996) Ionic mechanisms underlying synchronized oscillations and propagating waves in a model of ferret thalamic slices. *J Neurophysiol* 76:2049–2070.
17. Williams SR, Stuart GJ (2000) Action potential backpropagation and somato-dendritic distribution of ion channels in thalamocortical neurons. *J Neurosci* 20:1307–1317.
18. da Silva FH, van Lierop THMT, Schrijer CFM, van Leeuwen WS (1973) Organization of thalamic and cortical alpha rhythms: Spectra and coherences. *Electroencephalogr Clin Neurophysiol* 35:627–639.
19. Bollimunta A, Chen Y, Schroeder CE, Ding M (2008) Neuronal mechanisms of cortical alpha oscillations in awake-behaving macaques. *J Neurosci* 28:9976–9988.
20. Jones SR, et al. (2009) Quantitative analysis and biophysically realistic neural modeling of the MEG mu rhythm: Rhythmogenesis and modulation of sensory-evoked responses. *J Neurophysiol* 102:3554–3572.
21. Mathewson KE, Gratton G, Fabiani M, Beck DM, Ro T (2009) To see or not to see: Prestimulus alpha phase predicts visual awareness. *J Neurosci* 29:2725–2732.
22. Jones SR, et al. (2010) Cued spatial attention drives functionally relevant modulation of the mu rhythm in primary somatosensory cortex. *J Neurosci* 30:13760–13765.
23. Bollimunta A, Mo J, Schroeder CE, Ding M (2011) Neuronal mechanisms and attentional modulation of corticothalamic α oscillations. *J Neurosci* 31:4935–4943.
24. Rajagovindan R, Ding M (2011) From prestimulus alpha oscillation to visual-evoked response: An inverted-U function and its attentional modulation. *J Cogn Neurosci* 23: 1379–1394.
25. Lopes Da Silva FH, Storm Van Leeuwen W (1977) The cortical source of the alpha rhythm. *Neurosci Lett* 6:237–241.
26. Lopes da Silva FH, Vos JE, Mooibroek J, Van Rotterdam A (1980) Relative contributions of intracortical and thalamo-cortical processes in the generation of alpha rhythms, revealed by partial coherence analysis. *Electroencephalogr Clin Neurophysiol* 50:449–456.
27. Silva LR, Amitai Y, Connors BW (1991) Intrinsic oscillations of neocortex generated by layer 5 pyramidal neurons. *Science* 251:432–435.
28. Yamagishi N, Goda N, Callan DE, Anderson SJ, Kawato M (2005) Attentional shifts towards an expected visual target alter the level of alpha-band oscillatory activity in the human calcarine cortex. *Brain Res Cogn Brain Res* 25:799–809.
29. Foxe JJ, Snyder AC (2011) The role of alpha-band brain oscillations as a sensory suppression mechanism during selective attention. *Front Psychol* 2:1–13.
30. Worden MS, Foxe JJ, Wang N, Simpson GV (2000) Anticipatory biasing of visuospatial attention indexed by retinotopically specific–band electroencephalography increases over occipital cortex. *J Neurosci* 20:1–6.
31. Rihs TA, Michel CM, Thut G (2007) Mechanisms of selective inhibition in visual spatial attention are indexed by alpha-band EEG synchronization. *Eur J Neurosci* 25:603–610.
32. Palva JM, Palva S, Kaila K (2005) Phase synchrony among neuronal oscillations in the human cortex. *J Neurosci* 25:3962–3972.
33. Jensen O, Gelfand J, Kounios J, Lisman JE (2002) Oscillations in the alpha band (9-12 Hz) increase with memory load during retention in a short-term memory task. *Cereb Cortex* 12:877–882.
34. Busch NA, Herrmann CS (2003) Object-load and feature-load modulate EEG in a short-term memory task. *Neuroreport* 14:1721–1724.
35. Efron R (1970) The minimum duration of a perception. *Neuropsychologia* 8:57–63.
36. McAlonan K, Cavanaugh J, Wurtz RH (2008) Guarding the gateway to cortex with attention in visual thalamus. *Nature* 456:391–394.
37. Terman D, Bose A, Kopell N (1996) Functional reorganization in thalamocortical networks: Transition between spindling and delta sleep rhythms. *Proc Natl Acad Sci USA* 93:15417–15422.
38. Bonjean M, et al. (2011) Corticothalamic feedback controls sleep spindle duration in vivo. *J Neurosci* 31:9124–9134.
39. Bonjean M, et al. (2012) Interactions between core and matrix thalamocortical projections in human sleep spindle synchronization. *J Neurosci* 32:5250–5263.